Integration of Core Data for Calibrated Shaly-Sand Log Analysis

Jeff Hawkins, Senior Reservoir Engineer
Conoco Inc.

ABSTRACT

Routine and special core analysis, were used to calibrate shaly-sand log analysis models. Results from a calibrated Modified Simandoux model compare favorably with actual field performance and other 4th Grubb special core analysis data. The 4th Grubb reservoir is a deep, multi-sand interval, located in the San Miguelito Field in Ventura County, California. These sands are deep water, longitudinal turbidite deposits of Miocene and Pliocene age. Interbedded with these shaly sands are turbidite related silts and marine shales. A typical logging suite would include, gamma, dual induction, density and neutron. Occasionally sonic and dielectric logs were also run. Routine core analysis included porosity, permeability, grain density and saturations. Fourier transform infrared spectroscopy (FTIR), x-ray diffraction (XRD), thin sections, and scanning electron microscope (SEM) photomicrographs were used to identify clay type and clay content. Laboratory petrophysical measurements were made to determine the appropriate formation factor, saturation exponent and clay properties. Capillary pressure data were used to estimate irreducible water saturations (Swi), and relative permeability data were used to estimate fractional flows. Results of the log analyses and core analysis data were then compared to actual field performance.

INTRODUCTION

The case history presented illustrates how core analysis can help determine the parameters necessary for the various shaly-sand log analysis equations. Also illustrated is the importance of having core data to aid in calibration of log clay volume estimates. The paper also provides an example of how core analysis data and production data can be used to check the accuracy of the log analysis.

Available core analysis data included: routine porosity, grain density and permeability measurements, plus FTIR spectroscopy mineralogical analysis and complete petrographic analysis (XRD, SEM, and thin section photomicrographs). The FTIR spectroscopy measurements are commercially available as MINERALOG™ from Core Laboratories. Special core analysis included measurement of: core compressibility, core resistivity as a function of saturation and porosity, core conductivity as a function of water salinity (Co/Cw), capillary pressures, and relative permeabilities. The following sections discuss how the various analyses were integrated into the final log analysis.

GEOLOGY AND MINERALOGY

The 4th Grubb reservoir is made up of turbidite related arkosic sands deposited during the Late Miocene and Pliocene ages. The study of the rock mineralogy for the 4th Grubb reservoir was accomplished using XRD, FTIR spectroscopy, thin sections, and SEM.

Results from all the methods were consistent and indicated a complex and variable mineralogy. Ruessink and Harville (1992) also showed good agreement between FTIR and XRD mineralogical quantification, they also found the techniques to be fairly accurate. Their analysis of synthetic prepared samples of known composition showed that 90% of the data fell within 5 weight percent (wt%) error bands of the actual composition for both methods. However, they did indicate that depending on sample composition FTIR and XRD can both have substantial errors when quantifying rock composition.

Table 1 outlines the mineralogical composition of the rock indicating maximum, minimum, and average weight percent values for the constituents. In addition to the components listed, small amounts of pyrite and kaolinite were also identified in some samples. The main constituents of the rock are quartz and various amounts of the feldspars (Plagioclase, Albite, and Potassium (K) - feldspar). In general the rock contains less than 5 wt% carbonates, though streaks were encountered with a combination of greater than 30 wt% calcite and dolomite. Clays were also present with illite being the dominant clay. Small amounts, 1 to 2 wt%, kaolinite and chlorite were also seen.

Table I
4th Grubb Mineralogical Data
Weight % of Component

	Quartz	Chert	Plagioclase	Albite	K-Feldspar	Calcite	Dolomite	Illite + Smectite
Minimum	9.0	0.0	9.0	6.0	10.0	0.0	0.0	4.0
Maximum	46.0	23.0	46.0	20.0	26.0	22.0	34.0	42.0
Average	24.3	7.3	24.3	12.4	15.5	2.4	3.7	11.3

FTIR is unable to distinguish illite from smectite (Ruessink and Harville, 1992) and the weight percent of those clays is reported as a combined total. However from XRD we were able to determine that 80 to 90% of the illite plus smectite was illite. This high level of illite is expected due to the 13,000 foot depth and 240° F temperature of the rock (Bruce, 1984). The 4th Grubb reservoir sands were originally overpressured which is also consistent with smectite dehydration to illite (Bruce, 1984). Clay content in the rock varied from 4 to 42 wt% with an average value of 11.3 wt%. In thin section and SEM the clay was identified mostly as authigenic clays, with a small amount of detrital clay.

GRAIN DENSITY AND CLAY VOLUME

Whole cores or rotary drilled sidewall cores were cut in eight 4th Grubb wells. In all, over 350 feet of rock was sampled. As part of the routine core analysis, grain densities were measured. As suspected, due to the mineralogical complexity, there was some variability in the grain density. A low value of 2.59 and a high value of 2.72 g/cc were observed. The average value for the core data set was 2.65 g/cc with a standard deviation of only .02 g/cc, or less than 1% of the average. Even though there was substantial mineralogical variability in the rock, it was often self-compensating and the grain density remained near 2.65 g/cc. Grain densities calculated from composition were found to be unreliable. This is likely due to variable composition, hence variable density of many minerals occurring in these rocks. This range in density is particularly true of the clays

and feldspars. The average mineral grain densities combined with FTIR composition data predicted rock grain densities which were smaller than actual measured values.

Grain density and clay composition data from core can possibly be used to determine an average matrix density and an average clay density. Performing a volume balance on the core sample, excluding pore volume,

$$Vol_{sample} = Vol_{clay} + Vol_{matrix} \quad (1)$$

Where, VOL = Volume

Using the relationship of density, weight and volume the equation becomes,

$$\frac{WT_{sample}}{\rho_{sample}} = \frac{WT_{clay}}{\rho_{clay}} + \frac{WT_{matrix}}{\rho_{matrix}}$$

Where, WT = Weight
ρ = Density

Dividing through by the weight of the sample the equation becomes,

$$\frac{1}{\rho_{sample}} = \frac{WF_{clay}}{\rho_{clay}} + \frac{WF_{matrix}}{\rho_{matrix}}$$

Where, WF = Weight fraction

Substituting $1-WF_{clay}$ for WF_{matrix} the equation becomes,

$$\frac{1}{\rho_{sample}} = \frac{WF_{clay}}{\rho_{clay}} + \frac{1 - WF_{clay}}{\rho_{matrix}}$$

Finally factoring out WF_{clay} and rearranging terms we obtain:

$$\frac{1}{\rho_{sample}} = WF_{clay}\left(\frac{1}{\rho_{clay}} - \frac{1}{\rho_{matrix}}\right) + \frac{1}{\rho_{matrix}} \quad (2)$$

Examining the equation we see that the inverse of sample grain density plotted versus WF_{clay} is a straight line with intercept equal to the inverse of matrix density and slope equal to the difference between inverse matrix density and inverse clay density. Figure

1 shows the theoretical relationship for quartz and kaolinite. Of course this relationship only holds if both clay and matrix densities are relatively constant. Figure 2 shows the actual data plotted for the 4th Grubb grain density measurements and FTIR weight percent total clay measurements. Using all of the available data no obvious trend is seen, and certainly no linear relationship exists. There could be several reasons for this. The largest factor is probably the near equivalence of the matrix and clay densities, thus slight variations in either would obscure the trend. Another factor, as indicated earlier, could be the limited accuracy of the FTIR clay fraction measurements. The small standard deviation in grain density data for a wide range of clay content may indicate that the clay density and rock matrix density values are very similar. Clay densities for illite range from 2.5 to 2.9 g/cc (Deer et al, 1966; Edmundson and Raymer 1979) and in our case the illite and illite/ smectite combination may have an average grain density of 2.66 g/cc based on published density values. If the matrix grain density and clay grain densities are similar or rock grain density is relatively constant and independent of clay content, then effective porosity calculated from the density log should be accurate.

POROSITY

Helium porosities were measured on core samples at a nominal confining pressure of 400 psig, and were then corrected to reservoir confining stress. This was accomplished with core compressibility measured as part of the core analysis and repeat formation tester data, which was used to estimate reservoir pore pressures. The extra compaction of the rock at reservoir conditions was estimated to reduce core porosities 10%.

Whenever comparing core and log data, it is very important to adjust the data to the same depths. The core gamma and log gamma were used to depth adjust the core data to the appropriate log depth. Figure 3 shows how the core and log gamma ray readings were used to depth adjust the core data to the log depth.

Log porosities were calculated from the density log using the average measured grain density of 2.65 g/cc. Using this method, good agreement was seen between calculated log porosities and core porosities. For the cored intervals average corrected core porosity was 11.8% and average porosity estimated from the density log was 11.4%. Johnson and Linke (1977) also reported good correlation between density porosity and core porosity corrected for net overburden in a shaly sand. Figure 4 shows a crossplot of core porosity and porosity determined from the density log. Core plugs are one inch diameter samples while the logging tool is averaging over several feet, thus average values are a better means of comparison. Not surprisingly the largest differences between core and log data were seen where core grain density measurements indicated densities that were significantly different from 2.65 g/cc. Insufficient core data existed to attempt to determine appropriate grain densities for the different zones of the 4th Grubb. Using the density log for porosity determination in a shaly sand will only be valid when clay and matrix grain densities are similar, or clay content and thus rock grain density are relatively constant.

CLAY VOLUME

Weight percent clay from FTIR or XRD must first be converted to volume percent clay (V_{clay}) based on bulk volume before the data can be used in shaly-sand analysis.

$$WF_{clay} = \frac{WT_{clay}}{WT_{sample}}$$

Where, WF = Weight fraction
WT = Weight

Using the definition of density the above equation can be written in terms of density and volumes.

$$WF_{clay} = \frac{VOL_{clay} \times \rho_{clay}}{VOL_{sample} \times \rho_{sample}} \quad (3)$$

Putting the density terms on the other side of the equation and defining V'_{clay},

$$V'_{clay} = \frac{VOL_{clay}}{VOL_{sample}} = \frac{WF_{clay} \times \rho_{sample}}{\rho_{clay}} \quad (3)$$

substituting for VOL_{sample} as defined in equation (1) the equation becomes

$$V'_{clay} = \frac{VOL_{clay}}{VOL_{clay} + VOL_{matrix}} \quad (4)$$

Note: V'_{clay} does not include porosity

Now the definition of bulk volume is,

$$BV = VOL_{clay} + VOL_{matrix} + PV$$

Where, BV = Bulk Volume
PV = Pore Volume

subtracting pore volume from both sides,

$$BV - PV = VOL_{clay} + VOL_{matrix}$$

using this relationship to substitute for the denominator in equation (4), we obtain

$$V'_{clay} = \frac{VOL_{clay}}{BV - PV}$$

Factoring out bulk volume on the right side of the equation we obtain.

$$V'_{clay} = \frac{VOL_{clay}/BV}{1 - PV/BV}$$

The definitions of porosity and V_{clay} are,

$\phi = PV/BV$
$V_{clay} = VOL_{clay}/BV$

Where, ϕ = Porosity

plugging in these definitions the equation becomes,

$$V'_{clay} = V_{clay}/(1 - \phi)$$

Finally solving for V_{clay} and substituting for V'_{clay} in terms of densities and WF_{clay} from Equation (3) we obtain:

$$V_{clay} = \frac{WF_{clay} \times \rho_{sample} \times (1 - \phi)}{\rho_{clay}}$$

Many of the shaly-sand log analysis equations use clay volume (V_{clay}) or shale volume (V_{shale}) to adjust tool response for the presence of the clays. Shale is composed of clay and matrix material (quartz, feldspars, carbonates) of small grain size. Bound water, radioactive elements, and the differing grain density of clays affect the logging tool measurements. The problem with most of the V_{clay}/V_{shale} indicators is that they indicate 100% V_{clay} in the shale zone which is rarely the case. Hower et al. (1976) performed a detailed XRD study of shale cuttings from Gulf Coast formations. Their data indicates that average weight percent clay ranged only 55 to 68% in shale samples taken between 1850 to 5500 meters.

The neutron-density crossplot, SP, and density-sonic crossplot indicators in general will overestimate V_{clay} because they indicate 100% V_{clay} in the shale zone and are linear relationships. The Larionov transforms of the gamma-ray clay index are an exception. Though the Larionov transforms do indicate 100% V_{clay} in the shale zone, the transform

is non-linear and for a rock with a clay index of 30% the V_{clay} is 9.5%. In the case of the 4th Grubb, using neutron shale porosities picked from the log and "standard" densities (2.65g/cc for matrix and 2.54 g/cc for shale) crossplot clay volumes were on average 20% clay volume too high. Figure 5 shows a log trace section comparing the neutron-density crossplot clay volume with actual measured core data. The figure shows the danger of using uncalibrated estimates of clay volume. The core data indicated no discernable difference between the density of the clay and matrix, thus it appears the neutron- density crossplot technique is not useable for estimating clay volume in the 4th Grubb. The wells were drilled with an oil-based mud, thus no SP curves are available, and we were left with using the gamma ray log.

Although the radioactive potassium in the feldspar makes the gamma ray hot, we found the curve still useable. The gamma ray clean reading was merely a high value. The weight percent clay from FTIR was converted to V_{clay} using component grain density and sample porosity; these V_{clay} values were then used to calibrate the gamma ray estimate of V_{clay}. By selecting the appropriate clean and shale gamma ray values, a fairly good fit of core and log V_{clay} was obtained. Figure 6 shows a comparison of V_{clay} from FTIR measurements of core and V_{clay} estimated from the log gamma ray using the tertiary Larionov transform. Also shown is the core and log gamma ray traces and the excellent agreement between the core and log porosities for this interval. In general over the complete interval of more than 100 feet for which we had FTIR data there was good agreement between core and log gamma ray V_{clay}. At most depths in the interval shown in Figure 6 the V_{clay} estimates are very close, however between 13980 and 13990 the correspondence was off considerably. The difference at this depth may be due to changing matrix and clay properties in this complex rock. The previously mentioned problems with FTIR mineralogical identification could also be the cause. Note at these depths that the core and log gamma ray traces both indicate a "cleaner" reading, while FTIR data indicated a higher clay content. Examination of complete mineralogy of the samples gave no explanation, as there was not substantial decrease in K- feldspar or significant other mineralogical changes over the interval.

ESTIMATION OF LOGGING PARAMETERS

The various shaly-sand equations have parameters which must be determined prior to analysis. In addition to saturation and cementation exponents, such parameters as clay conductivity, bound water conductivity, or cation exchange capacity must be determined. Cementation exponent and saturation exponent for Archie's law (Archie, 1942) are determined from log-linear relationships of resistivity ratios at different porosities and saturations respectively. Unfortunately the shaly-sand equations make the relationships non log-linear.

However, a new parameter estimation technique (Maute et al, 1992) using error minimization allows one to determine the appropriate parameters for any of the shaly-sand equations. Kerig and Watson (1986) had previously used the same technique to analyze relative permeability data. Laboratory measured resistivities at different conditions of saturation and porosity enable one to determine the appropriate exponents and clay/shale properties for any of the shaly-sand equations. Statistics then indicate the appropriateness of the equation to the data. It should be noted that while resistivity versus saturation data is relatively easy to measure, there is a great deal of debate concerning the validity of the saturation distribution established in the core plug during

measurement (Baldwin and Yamanashi, 1989) and the effect of core preparation on clays (Worthington et al, 1986). We found our two electrode data to differ significantly from our four electrode data and recommend two electrode data not be used, because of end effects.

Laboratory measurements of resistivity versus porosity and saturation were made for several 4th Grubb samples. V_{clay}, calculated from weight percent clay, was available from FTIR. This data was then used with the parameter estimation technique to determine parameters for several of the common V_{clay}/V_{shale} shaly-sand equations. For most of the equations the data was best fit by setting the conductivity of the clay equal to zero. This in effect reduces the equation to Archie's equation. The equations which reacted like this were: Simandoux (Poupon, et al, 1967), Laminar (Poupon, et al. 1954), and Indonesian (Poupon and Leveaux, 1971). The equation which did the best job of fitting the laboratory data and coming up with reasonable parameters was the Modified Simandoux (Bardon and Pied, 1969). Clay conductivity estimated for the Modified Simandoux model (1.74 ohm-m) matched closely clay conductivity calculated from Co/Cw measurements (1.6 ohm-m). For the other equations it was necessary to set the value for clay conductivity and then with the value set, determine the saturation or cementation exponents. Maute et al. (1992) found the "a" parameter for calculation of formation factor to be a poorly fit parameter, they recommended that "a" be set equal to one, and that is what we did for our analysis. For ease of computation the saturation exponent was set equal to two for the non-linear shaly sand equations, which then become quadratic. Table 2 indicates the parameters for the various models determined from the laboratory data.

Table 2
Analysis of Laboratory Resistivity
Data Using Parameter Estimation

Method	m	n	Rclay
Archie	1.92	2.5	-
Simandoux	2.20	2.0*	1.6*
Modified Simandoux	2.10	2.0*	1.74

*Value was set

Our available core data enabled us to estimate clay volume in the rock, thus the models we evaluated were clay volume models and not the popular Waxman-Smits or Dual Water models. These models also deal with quantities such as shale and total porosity which were not readily available from our core data for use in calibration.

The calibrated shaly-sand equations were then used to perform log analysis on 4th Grubb wells. Figure 7 shows log analysis for several methods (using the laboratory calibrated parameters) for a section of the 4th Grubb in Grubb No. 396. Porosity and clay volume are shown along with saturations calculated using the calibrated Archie's, Simandoux, and the Modified Simandoux method. The calibrated Modified Simandoux method, which best fit the laboratory data, provides the lowest water saturations and as explained in the following section is most consistent with other special core analysis and production data.

USE OF SPECIAL CORE ANALYSIS AND PRODUCTION DATA

The validity of log analysis should be substantiated by comparison with other data. If a well generally produces water-free oil then the formation perforated must be at irreducible water saturation (Swi). The log calculated saturations for such a well can then be compared to the Swi from capillary pressure measurements. If a well initially produces with a water cut, then either water zones have been perforated or the formation is not at Swi. If no water zones are suspected then the surface water cut can be corrected to reservoir conditions using formation volume factors to determine the reservoir water cut (Willhite, 1986). Fractional flow curves calculated from laboratory measured relative permeability data can then be used to estimate the in-situ saturation. This saturation can be compared to the log calculated saturation.

In the case of the 4th Grubb, good agreement was seen between log analysis with the calibrated Modified Simandoux equation and special core analysis for the 4th Grubb. Figure 8 shows the log analysis for Grubb No. 366. Log determined saturations for Grubb No. 366 indicate saturations ranging from 25 to 45% in perforated intervals for this well that initially produced at a very low water cut. This value corresponded well with laboratory measured capillary pressure Swi values which ranged from 27 to 38%. An example laboratory measured oil-water capillary pressure curve of 4th Grubb core is shown in Figure 9.

Grubb No. 396, a recently completed well, came on with an initial water cut of around 50%, which converts to a reservoir fractional flow of water around 40%. Figure 10 shows a fractional flow curve calculated from laboratory measured oil-water relative permeability data of a 4th Grubb core sample. The 40% water fractional flow corresponds to a saturation of approximately 54%. Log analysis for Grubb No. 396, using the calibrated Modified Simandoux equation, indicates water saturations from 42 to 60%, with an average saturation for the perforated interval of 54%.

CONCLUSIONS

1. Mineralogical quantification from FTIR spectroscopy was consistent with results from XRD.

2. FTIR spectroscopy proved to be a relatively inexpensive means of quantifying clay type and clay fraction for the 4th Grubb reservoir. (Though FTIR does not distinguish between illite and smectite).

3. The 4th Grubb sands are mineralogically complex, and are mainly composed of a varying mixture of feldspars, quartz, carbonates, and clays.

4. No correlation was found between rock grain density and weight percent clay for the 4th Grubb reservoir. Average, grain density for the 4th Grubb was 2.65 g/cc.

5. Porosities calculated from a compensated density log compared favorably with core porosities.

6. Porosity and grain densities are necessary to convert weight percent clay from FTIR to clay volume fraction (V_{clay}) for shaly-sand analysis.

7. Uncalibrated V_{clay} estimates for the 4th Grubb were off considerably. The neutron-density crossplot technique overestimated clay volume on average by 20% clay volume.

8. In laboratory measurement of logging parameters (a, m and n) two electrode resistivity data differed significantly from four electrode resistivity data. Because of its susceptibility to end effects, two electrode data is not recommended.

9. Laboratory resistivity data were evaluated using a parameter estimation technique to determine shaly sand analysis parameters. The Modified Simandoux equation gave the best fit of the data.

10. Good agreement was seen between log analysis using the calibrated Modified Simandoux equation and results from laboratory capillary pressure and relative permeability measurements coupled with well production histories.

ACKNOWLEDGEMENTS

This work would not have been possible without the help of Brad Baker, André Bouchard, Tommy Ragland, and George Young of Conoco Inc. I thank them for their technical support and encouragement. I also thank the management of Conoco Inc., for permission to publish the paper.

SELECTED REFERENCES

Archie, G. E., 1942, The Electrical Resistivity Log as an Aid in Determining Some Reservoir Characteristics: Petroleum Technology.

Baldwin, B. A., and Yamanashi, W. S., 1989, Persistence of Nonuniform Brine Saturation Distribution in SCA Electrical Resistivity Study Core Plugs after Desaturation by Centrifuging: The Log Analyst, January- February, p. 45-48.

Bardon, C., and Pied, B., 1969, Formation Water Saturation in Shaly Sands: SPWLA 10th Ann. Log. Symp. Trans., paper Z.

Bruce, C. H., 1984, Smectite Dehydration-Its Relation to Structural Development and Hydrocarbon Accumulation in Northern Gulf of Mexico Basin: AAPG Bulletin, v. 68, no. 6, p. 673-683.

Edmundson, H. and Raymer, L. L., 1979, Radioactive Logging Parameters for Common Minerals: The Log Analyst, p.

Deer, W. A., Howie, R. A., and Zussman, J., 1966, AN INTRODUCTION TO THE ROCK FORMING MINERALS: Longman Group Limited, London, p. 260.

Hower, J., Eslinger, E. V., Hower, M. E., and Perry, A. P., 1976, Mechanism of burial metamorphism of argillaceous sediment: 1. Mineralogical and chemical evidence: Geological Society of America Bulletin, v. 87, p. 725- 737.

Johnson, W. L., and Linke, W. A., 1977, Some Practical Applications To Improve Formation Evaluation of Sandstones in the Mackenzie Delta, presented at the 6th Formation Evaluation Symposium of the Canadian Well Logging Society, Calgary, 19 p.

Kerig, P. D. and Watson, A. T., 1986, Relative Permeability Estimation from Displacement Experiments: An Error Analysis: SPE Reservoir Engineering, March, v. 1, p. 175-182.

Maute, R. E., Lyle, W. D., and Sprunt, E. S., 1992, Improved Data-Analysis Method Determines Archie Parameters From Core Data: JPT, January 1992, p. 103-107.

Poupon, A., Loy, M. E., and Tixier, M. P., 1954, A Contribution to Electrical Log Interpretation in Shaly Sands: Journal of Petroleum Technology, June, p. 27-34.

Poupon, A., Strecker, I., and Gartner, J., 1967, A Review of Log Interpretation Methods Used in the Niger Delta, SPWLA 7th Ann. Log. Symp., Paper Z.

Poupon, A., and Leaveaux, J., 1971, Evaluation of Water Saturation in Shaly Sands, SPWLA 12th Ann. Log. Symp., Paper O.

Ruessink, B. H., and Harville, D. G., 1992, Quantitative Analysis of Bulk Mineralogy: The Applicability and Performance of XRD and FTIR: SPE 23828, presented at the SPE International Symposium on Formation Damage Control, p. 533-546.

Whillite, G. P., 1986, WATERFLOODING: SPE Textbook Series V. 3., Richardson, Texas, p. 66.

Worthington, P. F., Toussaint-Jackson, J. E., and Pallatt, N., 1986, Effect of Sample Preparation upon Saturation Exponent in the Magnus Field, U.K. North Sea: The Log Analyst, January-February, p. 48-53.

ABOUT THE AUTHOR

Jeff Hawkins is a Senior Reservoir Engineer with Conoco in Oklahoma City. Previously he was at Conoco's Production Research facility where he conducted research in the area of special core analysis. He earned his BS in Chemical Engineering from the University of Nebraska and his MS in Petroleum Engineering from the University of Houston. He has also conducted research and patented methods for improving sweep efficiency in steamfloods and miscible floods. He is a member of the Society of Petroleum Engineers and the Society of Core Analysts and is a Registered Professional Engineer in Oklahoma.

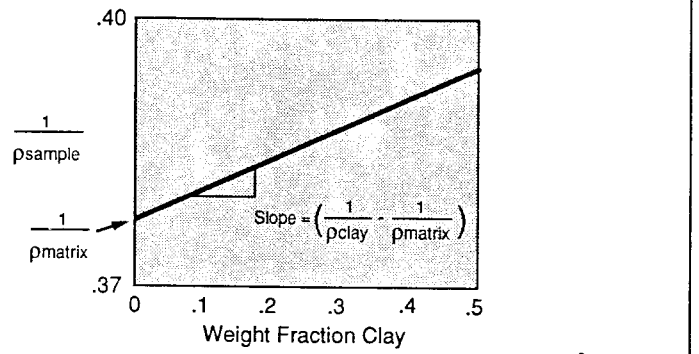

Quartz = 2.65 g/cm^3
Kaolinite = 2.42 g/cm^3

Figure 1

1 / (ρsample) vs Weight Fraction Clay
Theoretical Relationship

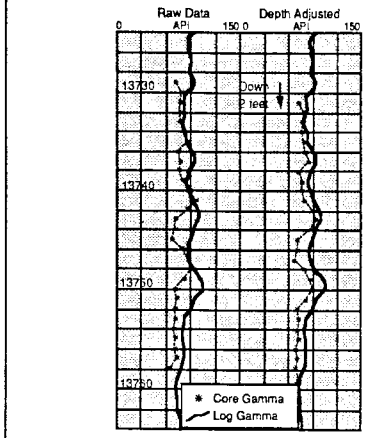

Figure 3

Use of Core Gamma to
Depth Adjust Core Data

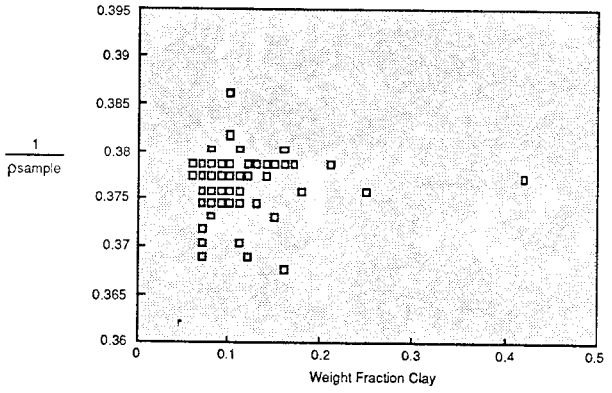

Figure 2

1 / (ρsample) vs Weight Fraction Clay
4th GRUBB CORE DATA

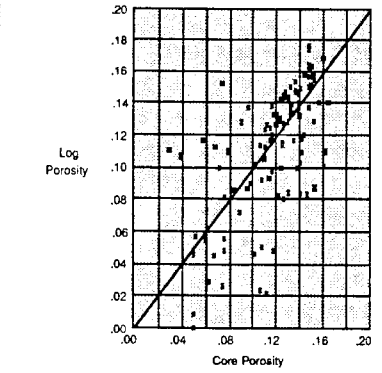

Figure 4

Log Porosity vs Core Porosity
4th GRUBB
GRUBB No. 396

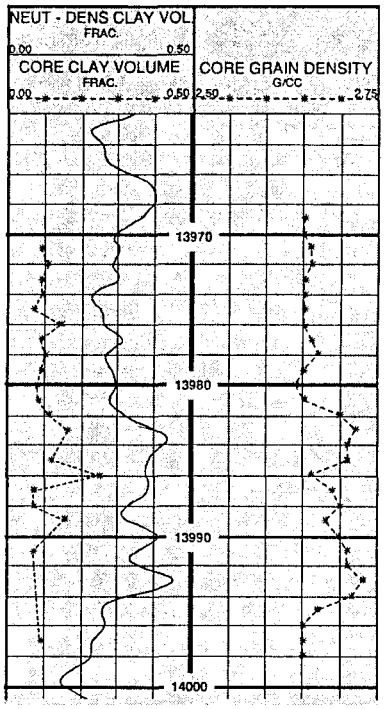

Comparison of Core Clay Volume and Clay Volume Estimated from Neutron-Density Log

Figure 5

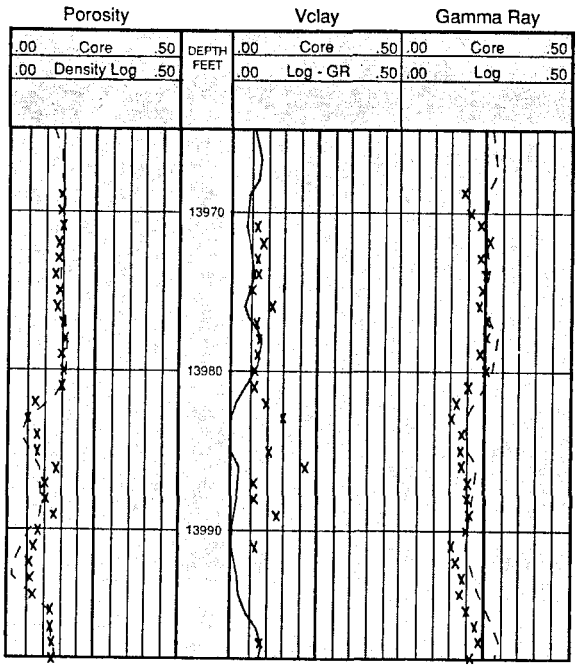

Comparision of Core and Log Results

Grubb No. 396

Figure 6

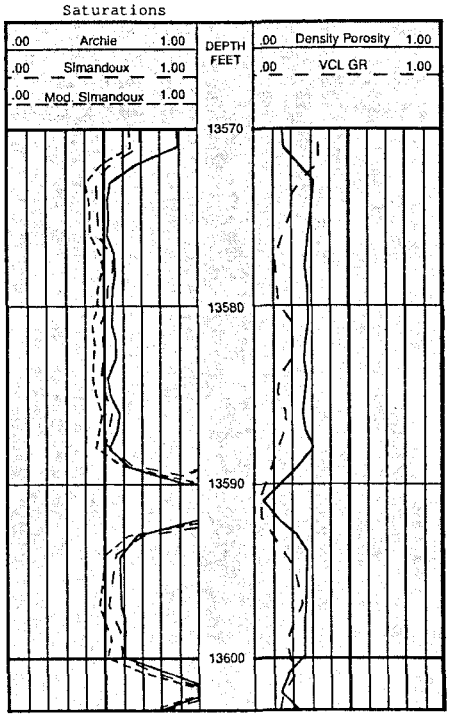

Comparison of Saturation Models

Grubb No. 396

Figure 7

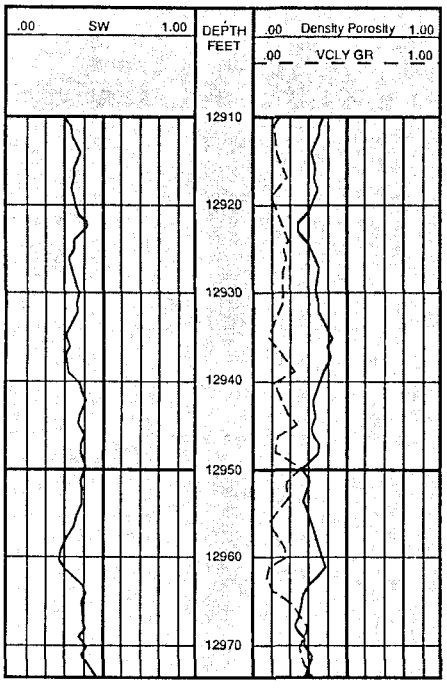

Modified Simandoux Log Analysis

Grubb No. 366

Figure 8

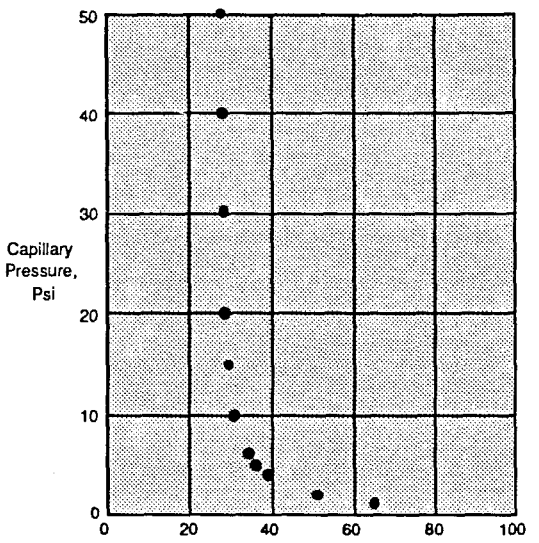

Oil - Water Capillary Pressure

4th Grubb Core Data
(Crude Oil; Temperature: 93 deg C)

Figure 9

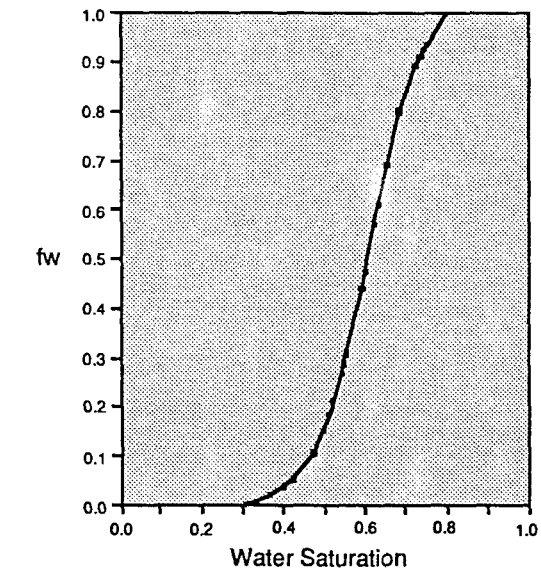

Fractional Flow Curve

4th Grubb Core Data
Grubb No. 353 RD

Figure 10